Published on 10 June 2019. Downloaded by National Institutes of Standards & Technology on 10/12/2022 10:12:13 PM.

Analyst

PAPER

View Article Online
View Journal | View Issue

Check for updates

Cite this: *Analyst*, 2019, **144**, 4219

Advances in age-dating of individual uranium particles by large geometry secondary ion mass spectrometry

Christopher Szakal, *[a] David S. Simons, [a] John D. Fassett[a,b] and Albert J. Fahey[c]

We present the ability to conduct single micrometer-sized uranium particle age-dating measurements on particles that are younger, smaller, and less enriched in ^{235}U content than previously reported. Specifically, we use large geometry secondary ion mass spectrometry (LG-SIMS) to precisely measure the $^{230}Th/^{234}U$ radiochronometer, combined with a systematic treatment of relevant parameters such as particle size, enrichment, and age, to achieve this development. We describe the necessary requirements for instrument background, interference rejection, abundance sensitivity, and other instrumental conditions that allow for this advance in single-particle uranium age-dating. We introduce the use of statistics developed by Feldman and Cousins to generate 95% confidence intervals in particle age, even when ^{230}Th daughter ions are not detected. For particles where counts are limited and are of identical isotopic signatures, we provide an option for aggregating individual measurements of single particles to reduce measurement uncertainty, as if the measurement had been performed on one larger particle. The methodology is validated on a range of certified reference materials and 'real-world' samples, ranging in age from 15 to 60 years, and on individual particles ranging in equivalent size from 0.6 to 6.8 micrometers. Additionally, we provide model age calculations for particles ranging in size from 1.0 to 3.0 micrometers across enrichments ranging from natural uranium to highly-enriched uranium and on ages ranging from 0 to 60 years. Experimental results compare well with the predicted model ages, providing realistic guidance for expectations of single micrometer-sized uranium particle age-dating measurements. The age-dating capabilities described herein are directly relevant to the International Atomic Energy Agency (IAEA) and its mission to safeguard nuclear materials and monitor member state nuclear programs.

Received 29th April 2019,
Accepted 6th June 2019

DOI: 10.1039/c9an00774a

rsc.li/analyst

Introduction

The International Atomic Energy Agency (IAEA) monitors facilities of its member states to assess their compliance with nuclear material safeguards obligations. Since 1991, the IAEA has used environmental sampling to detect the presence of nuclear materials as part of these inspections.[1–3] Inspectors use cotton wipes to swipe surfaces of equipment and structures at nuclear facilities and collect particles from nuclear material that has been processed at a given facility. The resulting samples are sent to the IAEA Headquarters for coding and distribution to the IAEA Network of Analytical Laboratories (NWAL), such as the Air Force Technical Applications Center (AFTAC) within the United States of America, for isotopic analysis. The isotopic analysis of individual particles is a powerful method that has become standard within the NWAL, especially for samples from uranium enrichment facilities.[4] After uranium particles are identified and isolated, isotopic analysis is usually performed either by thermal ionization mass spectrometry (TIMS) or secondary ion mass spectrometry (SIMS) to produce a measurement of the isotopic abundances of ^{234}U, ^{235}U, ^{236}U and ^{238}U. This information, if obtained from many individual particles in a sample, can provide a history of the various enrichment levels produced at a facility, rather than an average isotopic composition that a bulk measurement would provide. The particle information is used by IAEA data evaluators to verify the accuracy and completeness of the nuclear material declarations from each inspection site.

Beginning in 2005, the IAEA has repeatedly highlighted the need to determine the age of uranium particles collected *via* environmental sampling. This additional information would be extremely valuable to IAEA data evaluators and would reveal the date when the uranium from which a particle was derived was enriched or purified. Reports in the literature have shown preliminary feasibility to make such a measurement,[5–8] but the practical implementation of those methods has yet to be realized. As a result, the IAEA has continued to highlight age

[a]*Materials Measurement Science Division, National Institute of Standards and Technology, Gaithersburg, MD, USA. E-mail: cszakal@nist.gov*
[b]*Dakota Consulting, Inc., Silver Spring, MD, USA*
[c]*Corning Inc., Corning, NY, USA*

Published on 10 June 2019. Downloaded by National Institutes of Standards & Technology on 10/12/2022 10:12:13 PM.

determination of uranium and plutonium in environmental samples as one of its top priority R&D needs, up to and including 2018.[9] Such information would be critical to the IAEA to determine if enrichment activities occurred before or after a new treaty/agreement entered into force. Similarly, age-dating would also be indispensable in verifying compliance with the Fissile Material Cutoff Treaty, should that treaty go into effect.[10,11] A preliminary account of an advanced age-dating methodology and abbreviated description of this work aimed at meeting these safeguards needs was presented to the IAEA by AFTAC, in collaboration with the National Institute of Standards and Technology (NIST), in 2018.[12] In the present work, we systematically and thoroughly examine the age-dating measurement of uranium particles by large geometry secondary ion mass spectrometry (LG-SIMS) and demonstrate the practical feasibility of these measurements beyond what has previously been reported,[5–8] including a method to perform age-dating on small, young, and low-enriched uranium (LEU) particles.

Principles of radiochronometry and model age

Radiochronometers are well-known in the geochemistry community and several parent–daughter systems are potentially relevant to nuclear forensics. For age-dating of uranium particles, two systems are of particular interest: ^{234}U with a half-life ($T_{1/2}$) of 2.46×10^5 years decaying to ^{230}Th, and ^{235}U with a $T_{1/2}$ of 7.04×10^8 years decaying to ^{231}Th and subsequently to ^{231}Pa. Although the abundance of ^{235}U is typically about 2 orders of magnitude larger than ^{234}U, its half-life is nearly 3000 times longer, so the abundance of ^{231}Pa is expected to be about 30 times smaller than ^{230}Th. Therefore, we only consider the decay of ^{234}U in this work because the number of atoms of the decay daughter in a particle for the ^{235}U decay process will be even more limited.

The radioactive decay of a parent isotope to a daughter isotope that is itself radioactive is governed by the Bateman equation.[13] In the case of ^{234}U with decay constant $\lambda_{234} = 2.82 \times 10^{-6}$ per year decaying to ^{230}Th with decay constant $\lambda_{230} = 9.19 \times 10^{-6}$ per year, the equations are:

$$\frac{dN_{234}(t)}{dt} = -\lambda_{234}N_{234}(t), \quad (1)$$

$$\frac{dN_{230}(t)}{dt} = -\lambda_{230}N_{230}(t) + \lambda_{234}N_{234}(t), \quad (2)$$

where $N_{234}(t)$ and $N_{230}(t)$ are the number of atoms of ^{234}U and ^{230}Th at time t. The exact solution to these equations is

$$\frac{N_{230}(t)}{N_{234}(t_0)} = \left(\frac{\lambda_{234}}{\lambda_{230} - \lambda_{234}}\right)(e^{-\lambda_{234}t} - e^{-\lambda_{230}t}). \quad (3)$$

For the limiting condition where $t \ll 1/\lambda_{234}$ and $t \ll 1/\lambda_{230}$, eqn (3) simplifies to a linear ingrowth of the daughter isotope:

$$\frac{N_{230}(t)}{N_{234}(t)} \approx \lambda_{234}t, \quad (4)$$

where we assume that $N_{234}(t) \cong N_{234}(t_0)$ and $N_{230}(t_0) = 0$, *i.e.*, all ^{230}Th from the decay of ^{234}U that was present before the purification process has been completely removed. This is one of the 'model age' assumptions. Another assumption is that the parent–daughter system is 'closed', *i.e.*, neither parent nor daughter isotopes are lost to or gained from external sources. For a time t of 100 years, which is longer than any time of practical concern for individual uranium particle age-dating, the difference in the ratio calculation between the exact equation and the linear ingrowth approximation is only 0.03%, so we use the linear equation in this work to solve for the age $t = R/\lambda_{234}$ where R is the measured ratio of ^{230}Th to ^{234}U. A plot of eqn (4) on the time scale of the 'nuclear era' is shown in Fig. 1.

For very long times compared with the relevant half-lives, such as what occurs in uranium ores that are undisturbed over geologic time, a secular equilibrium is established whereby the number of ^{230}Th atoms that are ingrown from ^{234}U decay is balanced by the number of ^{230}Th atoms that decay. In that case, the left side of eqn (2) equals 0 and $N_{230}/N_{234} = \lambda_{234}/\lambda_{230} = 0.306$. A measurement of this value in an environmental particle of natural isotopic composition would likely indicate a geologic rather than anthropogenic source.

The concept of 'model age' as determined by eqn (4) is to be interpreted as the time since the most recent purification of thorium from uranium provided that the assumptions mentioned above are met. Such purifications of enriched uranium cannot be older than the middle of the 20th century. If uranium goes through a gaseous UF_6 stage during processing, such as enrichment by gaseous diffusion or centrifugation, the separation of thorium from uranium should be very high because thorium doesn't have a volatile fluoride phase at the operating temperatures of these processes. Likewise, any release of gaseous UF_6, such as from a storage cylinder, will reset the 'clock' provided that the solid residue containing ^{230}Th is not entrained with the gas. Given enough material, the determined model age should therefore be

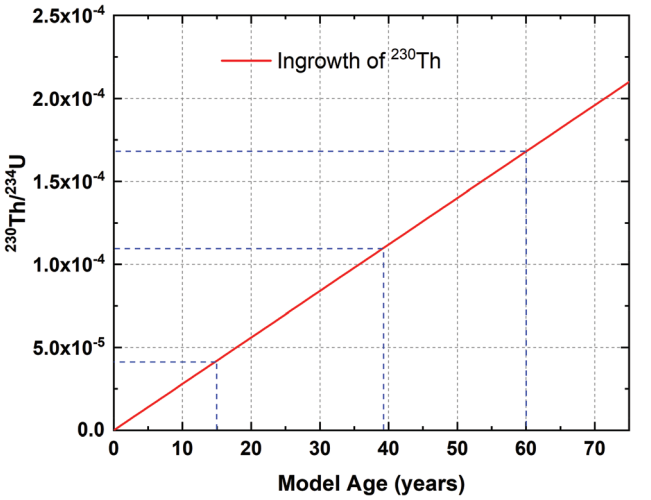

Fig. 1 Using eqn (4), a plot of ^{230}Th/^{234}U with $\lambda_{234} = 2.82 \times 10^{-6}$ per year *vs.* model age. Dashed blue lines drawn for approximate ages of particles analyzed in this work. For times that are consistent with secular equilibrium (>10^6 years), the ratio = 0.306.

This journal is © The Royal Society of Chemistry 2019

Published on 10 June 2019. Downloaded by National Institutes of Standards & Technology on 10/12/2022 10:12:13 PM.

considered the oldest possible 'true' age since the last processing of the uranium material took place because it is plausible that some operations may not completely remove all existing ^{230}Th. An example of the degree of purification required to make meaningful measurements in this system can be illustrated thusly: if uranium ore was processed so that 99.9% of the ingrown ^{230}Th was removed, the model age would still be greater than 100 years.

Challenge of particle measurements

Both the ^{234}U to ^{230}Th and ^{235}U to ^{231}Pa radiogenic systems mentioned above have been used for determining model uranium ages for bulk amounts of material,[14,15] but micrometer-sized particles have a very limited amount of material available for analysis. Previous attempts at making age-dating measurements on uranium particles have come to a consistent conclusion that measurements could only be made on particles that are sufficiently large, enriched, and/or old enough to yield the necessary measurement sensitivity.[8,11] These conclusions make conventional sense: one can only measure what can be counted. Since it isn't enough to just detect the ^{230}Th, but it is also necessary to make useful quantitative measurements, traditional metrics have dominated previous discussions. It is usually assumed that a minimum relative age uncertainty is required for a measurement to be useful, and this uncertainty is controlled by the Poisson statistics of the number of ^{230}Th ion counts that are acquired. IAEA environmental collections from enrichment plants generally obtain small particles in the micrometer size range. A 1 μm sphere of chemically purified UO_2 contains approximately 10^{10} uranium atoms. If we assume a ^{234}U/^{235}U ratio of about 0.01 (a typical value across a range of enrichment levels), a 100% duty cycle (all sputtered ions are counted), and a ^{230}Th detection efficiency (conversion of sample atoms to counted ions) of 0.7% (a similar number to what others have reported),[8] then an arbitrarily chosen 'detection limit' of 10 counts of ^{230}Th would require at least 1400 ^{230}Th atoms to be present in a given particle. As Table 1 shows, 1400 atoms of the daughter isotope are not available to be counted in a 1 μm spherical particle up to more than 50 years of age for any uranium enrichment less than 10% ^{235}U. The metrics are more favorable to measure the ^{230}Th in a 3 μm particle, but with conditions still slanted to only make measurements that fit the higher enriched and older uranium source material. In contrast, we present for the first time, a detailed methodology to make meaningful age-dating measurements constrained by well-defined uncertainty intervals on individual uranium oxide particles even if the counts of ^{230}Th are below any conventional detection threshold.

Table 1 Charts of ^{230}Th atoms present for a range of ^{235}U enrichments and ages for 1 μm and 3 μm diameter particles. Blocks highlighted in yellow indicate conditions allowing detection of at least 10 ions; assumptions for the calculation: a ^{234}U/^{235}U ratio of 0.01, a 100% duty cycle, and a ^{230}Th detection efficiency of 0.7%

Age (years) / ^{235}U (%)	0.5	1	2	5	10	50
1 μm UO_2 particle						
1	1	3	6	14	28	140
2	3	6	11	28	56	280
5	7	14	28	70	140	700
10	14	28	56	140	280	1400
20	28	56	112	280	560	2800
50	70	140	280	700	1400	7000
90	126	252	504	1260	2520	12 600
3 μm UO_2 particle						
1	38	76	151	378	756	3780
2	76	151	302	756	1512	7560
5	189	378	756	1890	3780	18 900
10	378	756	1512	3780	7560	37 800
20	756	1512	3024	7560	15 120	75 600
50	1890	3780	7560	18 900	37 800	189 000
90	3402	6804	13 608	34 020	68 040	340 200

Experimental section

LG-SIMS

The instrument employed to make the measurements described in this work is a CAMECA IMS-1270E7/1280 (Cameca Instruments, Inc., 5470 Nobel Dr, Fitchburg, WI, USA) large geometry secondary ion mass spectrometer (LG-SIMS).[16] It was originally acquired as an IMS-1270 and was upgraded with new electronics and computer control to make it as compatible as possible with the CAMECA IMS-1280. The procedures described herein, although intended for the specific instrument located at NIST, can be implemented on any LG-SIMS instrument.

Previous reports of uranium particle age-dating with SIMS have described efforts with both LG-SIMS and smaller geometry SIMS instruments.[5–8] As some have stated elsewhere,[8] the smaller geometry instruments cannot provide an adequate combination of sufficient mass resolving power to reject isobaric interferences with uranium and/or thorium along with sufficient ion transmission to efficiently measure the count-limited ^{230}Th for this radiochronometer. With the settings detailed below, LG-SIMS can routinely be employed with a mass resolving power greater than 3400 m/Δm, where Δm is the full width at 10% of peak maximum, while transmitting approximately 90% of the secondary ions through the mass spectrometer. This arrangement is ideally suited for measuring the ^{234}U and ^{230}Th with high sensitivity in single micrometer-sized particles while rejecting all common interfering molecular ions with either measured nuclide.

Instrumental setup

The NIST LG-SIMS instrument is fitted with a dual-polarity Hyperion II RF plasma oxygen source from Oregon Physics (Beaverton, OR, USA). From this source, a 13 keV O^- primary ion beam is directed through the primary ion column *via* a 3 mm primary beam mass filter aperture and a 200 μm 'lens 4' aperture to produce a Köhler illumination spot on the sample. The negative primary ion beam is used to minimize the effects

Published on 10 June 2019. Downloaded by National Institutes of Standards & Technology on 10/12/2022 10:12:13 PM.

of charging for larger uranium particles. With this configuration, the 4 : 1 demagnification of the 'lens 4' aperture produces an approximately 50 × 70 μm elliptical spot size on the sample held at +10 kV (net 23 keV impact energy). Primary ion currents measured in the primary ion column Faraday cup range from 15 to 90 nA for age-dating measurements, depending on particle size. Additional primary column lens and deflector settings used in this study are available upon request.

The secondary spectrometer settings are adjusted to produce 90% ion transmission at or better than the mass resolving power mentioned above as determined by a high-resolution scan of ^{235}U from a test particle. Specifically, the entrance slit is 175 μm, contrast aperture is 400 μm, energy slit bandpass is 50 eV, the exit slit is 250 μm, the field aperture (FA) is 6 mm, the maximum field-of-view determined by the transfer optics is 50 × 50 μm gated to 75% by the FA, and beam shaping is in the XY mode. These slit settings are narrow enough to exclude the pertinent spectral interferences[17] while minimizing the reduction in ion transmission. Importantly, the peak scans of each isotope reveal sufficient flat-top regions for stability in ion counting even with small magnetic field variations. Secondary ions are pulse-counted with the monocollector electron multiplier (EM) at a 75 mV threshold and a measured dead time of 27.5 ns.

A cycle is defined as an electronically varied timing sequence for measuring multiple mass/charge ratios at distinct magnetic fields, where counts are acquired in the electron multiplier for a given dwell time (dt), each separated by a wait time (wt) for stabilizing the magnetic field. For the age-dating measurement of 20 total cycles, each cycle consists of measuring: $^{207}Pb^{23}Na$ (2.00 s dt, 2.00 s wt), ^{230}Th (20.00 s dt, 0.96 s wt), and ^{234}U (2.00 s dt, 0.96 s wt). The $^{207}Pb^{23}Na$ peak position is located 0.0675 amu below the calibrated ^{230}Th position to monitor a potential molecular ion (such as $^{207}Pb^{23}Na$) that could bias the counting of ^{230}Th if the interfering signal was very large. The total acquisition time for 20 cycles is approximately 570 s, of which approximately 70% is used to measure the ^{230}Th signal, resulting in only a small duty cycle penalty for peak switching with the monocollector EM compared with the use of multicollector EMs. We have not investigated the use of the multicollector detector array on the LG-SIMS for age-dating. Its main advantage would be the collection of ^{230}Th counts from the remaining 30% of the duty cycle, but the other issues discussed later in this section would need to be carefully considered to determine if a multicollector assembly could be used to conduct age-dating measurements at the quality reported herein.

Blank measurements of 20 cycles are performed separately on a clean area of the sample planchet at least 1 mm away from a previously analyzed particle, with each cycle consisting of: $^{207}Pb^{23}Na$ (20.00 s dt, 2.00 s wt), ^{230}Th (20.00 s dt, 0.96 s wt), ^{234}U (2.00s dt, 0.96 s wt) after a 200 s pre-sputter (total acquisition time is approximately 1050 s). Monitoring a background channel during a particle analysis would waste valuable sample and is hence performed separately. The background runs measure the electronic noise of the detection system under age-dating analysis conditions as well as the effect of scattered ions from the substrate material (typically carbon).

Uranium isotopic abundance measurements are generally desired for the individual particles in addition to the age-dating measurements. They may be incorporated as part of an initial SIMS screening of a particle dispersion to determine the locations of uranium-bearing particles and to select which would be appropriate for age-dating. However, if isotopic analysis is performed after the age-dating measurement, uranium hydride species that interfere with ^{236}U are usually reduced substantially.[18] It is also helpful to monitor ^{232}Th as part of the isotopic abundance measurement because it could indicate the presence of a mineral source of uranium within the analysis area, or an incomplete purification of isotopically natural uranium – observations that can help to explain abnormally high $^{230}Th/^{234}U$ ratios.

Samples and materials

Particle reference materials for age-dating are produced by dispersing Certified Reference Material (CRM) uranium oxide particles onto 25 mm diameter carbon planchets at an areal density that allows sufficient separation between adjacent particles (at least 200 μm). This procedure was used for the preparation of planchets of the following CRMs across the full range of isotopic compositions: U005a, U010, U030a, U100, U350, U500, U750, U900, and U970, all of which have known purification (enrichment) histories (see Table 2).[19] Particles of uraninite from Topsham, Maine were prepared in the same manner. Additionally, two separate highly enriched uranium (HEU) metal materials from a Nuclear Forensics International Technical Working Group (ITWG) exercise were analyzed as an example of a more challenging 'real-world' type of sample.[20] Briefly, each uranium metal material, denoted 'Sample A'/cast date of May 2003 and 'Sample B'/cast date of January 2004, was separately cast from slightly different HEU source materials. Particles for this study were collected by swipe sampling of saw-cut pieces with additional details of the samples in Table 2. The uranium in the particles was likely in an oxide form when the particles were analyzed because uranium metal is known to oxidize readily.

Interelement calibration

The SIMS relative sensitivity factor (RSF) is a measure of the relative efficiency of converting sputtered atoms to detected ions between two different elements. For the isotopes of interest in this work, the RSF is defined by the equation:

$$RSF_{ThU} = \frac{N_{230}{}^{+}/N_{234}{}^{+}}{N_{230}/N_{234}}, \quad (5)$$

where $N_{230}{}^{+}/N_{234}{}^{+}$ is the measured $^{230}Th^{+}/^{234}U^{+}$ ratio. Daily calibrations of the RSF between thorium and uranium are performed with the above measurement conditions on several single U_3O_8 particles from a dispersion of CRM U900 particles. This material is ideal for the calibration procedure since the

 This journal is © The Royal Society of Chemistry 2019

Published on 10 June 2019. Downloaded by National Institutes of Standards & Technology on 10/12/2022 10:12:13 PM.

Table 2 Best-known purification dates for each uranium material used in this study, along with ^{235}U and ^{234}U atom percent, and analysis date information

Material	Best-known purification date	^{235}U atom%	^{234}U atom%	Analysis date	Age at date of analysis (years)
U005a	27-July-1981[a]	0.5064	0.0034	19-Apr-2018	38.6[c]
U010	5-June-1958	1.0037	0.0054	17-Apr-2018	59.9
U030a	27-July-1981[a]	3.0404	0.0278	13-Dec-2017	38.6[c]
U100	8-Jan-1959	10.190	0.0676	20-Nov-2017	58.9
U350	24-Jun-1958	35.190	0.2498	15-Nov-2017	59.4
U500	28-Nov-1962[a]	49.696	0.5181	11-Jul-2017	54.6
U750	20-Aug-1958	75.357	0.5923	26-Jun-2017	58.9
U900	24-Jan-1958	90.196	0.7777	12-Apr-2018	60.3
U970	23-Mar-1965	97.663	1.6653	30-Nov-2017	52.7
'Sample A'	22-May-2003[b]	92.929	0.999	17-Aug-2018	15.3
'Sample B'	14-Jan-2004[b]	91.428	0.972	27-Aug-2018	14.6

[a] Denotes shipment date of the original material, which is extremely close to the assumed purification date when compared with process notes of similarly made materials.[19] [b] Denotes known casting date of uranium metal. [c] Denotes model age that is not identical to the best-known purification date because of incomplete separation of Th during the material preparation.[21]

high age and high ^{234}U abundance allow sufficient ions of the daughter isotope to be counted to locate the centroid of the peak and to achieve good counting statistics. The RSF is calculated by combining eqn (4) and (5) to give the following equation:

$$RSF_{ThU} = \frac{N_{230}{}^{+}/N_{234}{}^{+}}{\lambda_{234} t}, \quad (6)$$

where t is the known purification age of U900 at the time of the measurement. For an unknown sample, its model age t is calculated by rearranging eqn (6) to give:

$$t = \frac{N_{230}{}^{+}/N_{234}{}^{+}}{RSF_{ThU}\lambda_{234}}. \quad (7)$$

Multiple measurements over a long term are used to determine an RSF value and a conservative uncertainty based on the long-term variability of the measured values. For this age-dating measurement calibration, the primary ion current is adjusted to consume more than 50% of a particle during a 20 cycle analysis and this procedure usually produces an initial $^{234}U^{+}$ count rate in the range of 10 000 counts per second. Fig. 2 shows a plot of how the Th/U ratio changes as a function of sputter time within an individual U900 particle. The ratio increases by about 10% as the particle is consumed by sputtering. Therefore, it is important to have a consistent approach to measuring the RSF within standard particles and to maintain this approach when measuring 'unknown' particles. From data in Fig. 3, the long-term Th/U RSF value is 0.673 with a relative standard deviation of approximately 3.6% across more than 300 measurements. Empirically, sputtering through and subsequently past the maximum ^{234}U signal within a particle until the ^{234}U decays to approximately 2/3 of its maximum count rate provides a high level of RSF consistency.

The individual particle RSF measurement variability demonstrated in Fig. 3 can be attributed to at least two factors that are both related to the challenges of making precise measurements on single particles: (1) the number of acquired ^{230}Th counts in each particle is inherently low, contributing to most of the overall RSF uncertainty, and (2) the trending of the RSF as shown in Fig. 2 varies slightly with particle size, and the U900 standard particles are not all of uniform particle size. Because age-dating measurements are desired to be made on a range of particle sizes, the RSF uncertainty of ±3.6% (±7.1% expanded uncertainty) as measured from the Fig. 3 data is critical for not underestimating the overall model age uncertainty for unknown particle measurements.

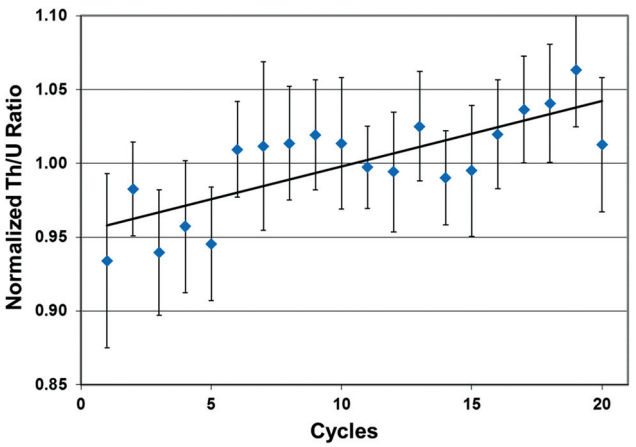

Fig. 2 Change of the $^{230}Th/^{234}U$ ratio cycle-to-cycle within an analysis of U900 particles; results from 20 independent particle measurements were combined by normalizing each to its average ratio and averaging the results; error bars are 95% confidence limits (CLs).

Interference rejection

We consider whether potential sources of counts at m/z 230 other than those produced by ^{230}Th ions will result in a measurable signal. One possible contribution is from molecular or cluster ions that occur at the same nominal mass as the isotope of interest. These types of ions are known to be produced during SIMS analysis from other elements that are present in the sample. Such considerations are important because environmental uranium particle samples often

Published on 10 June 2019. Downloaded by National Institutes of Standards & Technology on 10/12/2022 10:12:13 PM.

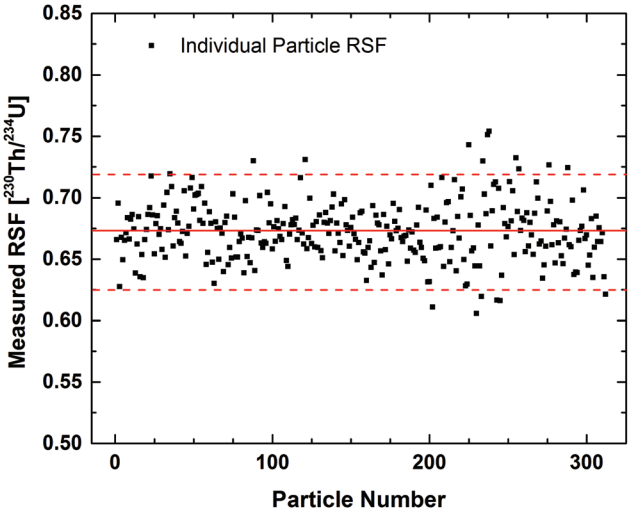

Fig. 3 Plot of Th/U relative sensitivity factor (RSF) for 310 individual particle measurements of CRM U900 taken over more than one year. The solid red line is the average Th/U RSF of 0.673 for all measurements with the dotted lines representing ±7.1% expanded uncertainties based on 1.96× the standard deviation of the individual data.

contain additional elements, and because the actual ^{230}Th signal from these samples is often very small. At *m*/*z* 230, potential cluster ions that are closest in mass to ^{230}Th (*m*/*z* 230.0331) and consist of a small number of atoms are those containing lead ($^{206}Pb^{12}C_2$, $^{207}Pb^{23}Na$, and $^{206}Pb^{24}Mg$). Of these, $^{206}Pb^{12}C_2$ is the closest at Δm = 0.0587 amu below ^{230}Th, requiring a resolving power of 3920 m/Δm to separate the two peaks. However, we are not concerned here with resolving the interfering peak, but rather with the contribution of the high-mass tail of the interfering peak at the mass of ^{230}Th where the measurement of the daughter isotope is made. To illustrate this point, Fig. 4 shows a mass scan of a uraninite mineral particle in the region of *m*/*z* 230, taken under similar slit conditions as used for the age-dating measurements. The scan shows peaks due to $^{206}Pb^{12}C_2$ and to ^{230}Th. The former peak is likely formed from radiogenic lead that is intrinsic to the mineral sample combined with carbon from the graphite substrate. Superimposed on the two peaks in red and blue dotted lines are peak scans of ^{234}U taken from a similar particle under the same conditions and scaled in mass and intensity to fit the peaks in the figure to show their extended peak shapes in the overlap region. This figure demonstrates that the extended high-mass tail of the $^{206}Pb^{12}C_2$ peak doesn't overlap the ^{230}Th mass position even after the signal from the tail has decreased by a factor of more than 1000 from the molecular peak signal, indicating that the interfering peak would need to be much more than 1000 times greater than the ^{230}Th signal before it would make a measurable contribution to that signal. During age-dating measurements, we routinely monitor the signal at $^{207}Pb^{23}Na$ (0.0675 amu below ^{230}Th) and have measured ratios as high as 80 000 : 1 between this potential interference peak and the ^{230}Th signal, indicating the degree of interference rejection provided by these analysis conditions. The only potential interference peaks that would be closer than $^{206}Pb^{12}C_2$ are complex molecular ions consisting of many light element species, *e.g.*, $C_{16}H_6O_2^+$ (*m*/*z* 230.0368), that would be unlikely to form and survive under high current density SIMS conditions. Thus, the spectrometer conditions selected for LG-SIMS analysis will reject all potential interfering species at the ^{230}Th mass position for practical purposes while maintaining a spectrometer transmission of about 90% relative to fully opened slit conditions.

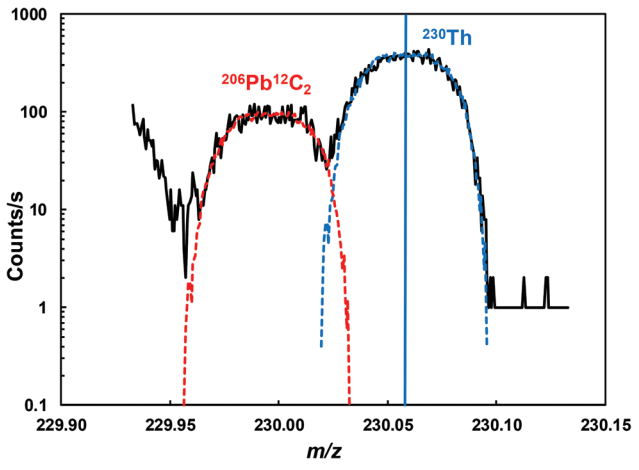

Fig. 4 Mass scan from uraninite particle of the $^{206}Pb^{12}C_2$ molecular ion peak at nominal *m*/*z* 230 and the ^{230}Th peak, which is 0.0587 amu above the interference peak; *y*-axis is a log scale, showing that the interference peak tail does not overlap the ^{230}Th peak position; superimposed peak shapes are from a mass-shifted scan of the ^{234}U peak; mass resolving power at 10% of peak maximum is 3680 m/Δm.

Abundance sensitivity

Another potential signal source at the ^{230}Th mass position is the scatter tail of the major uranium peak that will be 5 amu above the daughter peak of interest in the case of HEU. Scattering of ions within the mass spectrometer flight path from high-abundance isotopes can potentially produce significant background at other mass positions. The magnitude of these stray signals relative to the major peak signal defines the abundance sensitivity as a function of the separation from the major peak. To assess this contribution, we analyzed CRM U900 particles (0.7777% ^{234}U, 90.196% ^{235}U) in the LG-SIMS by sputtering with an O^- ion beam under similar conditions used for age-dating to produce a count rate of approximately 10^5 counts per second for ^{234}U. We measured the ratios of signals at half-mass positions to the ^{234}U signal from *m*/*z* 229.5 to *m*/*z* 234.5, interpolated the ratios to the integer mass positions, and normalized the ratios to the ^{235}U signal. The results are shown in Table 3. The scatter tail from ^{235}U at *m*/*z* 230 is very small but not zero. For U900, the ratio of the tail signal to ^{234}U is about 1.2×10^{-7}. Under the age-dating conditions described in this paper, this ion ratio corresponds to an apparent model age of about 3 weeks. This scatter ratio could be subtracted as a background, but it will be a negligible source of uncertainty for any practical particle measurements.

This journal is © The Royal Society of Chemistry 2019

Published on 10 June 2019. Downloaded by National Institutes of Standards & Technology on 10/12/2022 10:12:13 PM.

Table 3 Interpolated scatter ratio from ^{235}U peak signal using an exponential fit under the conditions described in the Instrumental Setup section

Nominal mass	Scatter ratio
234	2.4×10^{-7}
233	6.2×10^{-8}
232	1.6×10^{-8}
231	4.0×10^{-9}
230	1.0×10^{-9}

Detector background

Both the ^{230}Th channel and the monitored $^{207}Pb^{23}Na$ interference channel are used for blank measurements that are ideally made under standard age-dating analysis conditions on a clear portion of the sample planchet if such a region is available. Total blank counts are added from the combination of both channels (800 total seconds in a measurement). The average measured counts for the blank runs is typically in the range of 0.002 counts per second averaged over 10 000 total seconds of blank measurements. The electronic background (dark noise) of the electron multiplier can be measured over much longer times without sputtering a sample by using the 'Scan Parameters' function of the LG-SIMS for an overnight acquisition and the results have been consistent with the active background measurements. An accurate measurement of the average background is required since less than 10 counts of ^{230}Th are often measured, and if the particle is small, young, or of low enrichment, the measured counts may even be zero but the measurement may still yield useful data (see Discussion below).

Results and discussion

Treating low-count data

From a nuclear forensics standpoint, the detection of very 'young' enriched uranium would be of great significance because it could indicate, for example, that a facility had violated an international agreement to cease enrichment activities after a specified recent date. Previous approaches to age-dating of particles had indicated that the measured counts of ^{230}Th must exceed a specified minimum value for the measurement to be considered valid.[8,11] This criterion is equivalent to requiring a minimum relative age uncertainty. Imposing this requirement might reject the data from particles even though they produced high signals of ^{234}U. However, in the hypothetical situation mentioned above, the confidence limits (CLs) on the model age can provide constraints that could still be highly relevant even if the relative age uncertainty was large. In particular, the upper CL on the model age could be useful in indicating whether the data provided evidence of a treaty violation.

Ion counting uncertainties in mass spectrometry are generally dominated by Poisson statistics at low count rates, and the statistics of low-level counting in the presence of background has been considered in other scientific areas. An approach by Feldman and Cousins from the field of high-energy particle physics has a direct correspondence to the present work.[22] These authors consider Poisson processes in the presence of background and use a construction method based on frequentist statistics to generate tables of 68.3%, 90% and 95% confidence intervals for various combinations of observed counts from 0 to 20 and average background values from 0 to 15. We have incorporated their calculation method into a procedure for determining 95% CLs on age when the counts of ^{230}Th are low or zero. In practice, the average background count rate is determined as described previously, and the estimated background counts of ^{230}Th for an analysis are calculated based on the time over which ^{230}Th counts are recorded, typically 400 s. From the recorded counts and the estimated background counts, the 95% CLs on counts are determined, either by interpolation of the Feldman–Cousins tables or by a spreadsheet macro that has been developed. The CL constraints on model age are then calculated by dividing the 95% lower and upper count limits by the ^{234}U counts normalized to the same acquisition time and applying eqn (7) to the resulting ratios. In this approach, the ^{234}U counts are an inverse scaling factor for the CL constraints on model age, and the CLs can be small if the ^{234}U counts are high, even if very few or zero counts of ^{230}Th are recorded.

Model studies

To illustrate the low-count treatment principles described in the previous section, we provide calculated model age 95% CLs for three relevant environmental particle sizes, five uranium enrichment levels, and seven distinct particle ages in Table 4. The chart in Table 4 is additionally color-coded according to the expected utility of the individual particle age-dating measurement results. Color categories for confidence interval widths are defined as: red – large interval widths that cannot provide a useful restriction of possible particle ages, yellow – interval widths that can exclude very young and/or old possible particle ages, green – narrow interval widths that can exclude large ranges of possible particle ages within the nuclear era, and blue – extremely narrow interval widths of 4 years or less that can provide possible particle ages with sufficient confidence to answer questions of interest to the nuclear safeguards community. Several general observations can be made from these model age calculations: (1) for 1 μm particle sizes, age-dating results for natural (0.72%) and LEU (3.0%) materials do not yield CLs that provide any useful information about the environmental particles of interest, (2) as the enrichment and specifically the ^{234}U content of a particle increases, CLs become sufficiently narrow to provide potentially useful information about a given facility, even for 1 μm particle sizes, (3) for particles as small as 2 μm, CLs become sufficiently small to provide potentially useful information even for 20% enriched and LEU materials, (4) for particles in the 3 μm size range, age-dating constraints on individual particles yields potentially useful data from LEU to HEU at any age, and may be able to help answer questions of interest for natural material as well. These general observations should not be surprising – the utility of single particle age-dating is

Published on 10 June 2019. Downloaded by National Institutes of Standards & Technology on 10/12/2022 10:12:13 PM.

Table 4 Model age 95% CL calculations (in years) for a range of uranium particle sizes, enrichments, and ages, color-coded to the expected utility of the individual particle analysis results; assumptions used for the calculations: solid spherical particles of UO_2, RSF = 0.673 (from Fig. 3), uranium ion efficiency = 1%, 70% ^{230}Th duty cycle, Feldman Cousins CL calculation as described in the text plus propagated RSF uncertainty (Fig. 3) up to approximately 500 ^{230}Th counts, then Gaussian uncertainties used at 1.96× standard deviations; ^{234}U atom percent for each enrichment are in Table 2 for each corresponding CRM, with the exception of the 0.72% natural material (^{234}U of 0.0054%) and the 20% enriched material (^{234}U of 0.1246% for CRM U200). Model age is in years and 95% LL and 95% UL are lower and upper 95% CLs in years

1.0 μm particle				2.0 μm particle				3.0 μm particle			
^{235}U	Model age	95% LL	95% UL	^{235}U	Model age	95% LL	95% UL	^{235}U	Model age	95% LL	95% UL
0.72%	0	0.00	451.93	0.72%	0	0.00	56.52	0.72%	0	0.00	16.75
	1	0.00	451.93		1	0.00	56.52		1	0.00	16.75
	2	0.00	451.93		2	0.00	56.52		2	0.00	16.75
	5	0.00	451.93		5	0.00	56.52		5	0.00	23.13
	15	0.00	451.93		15	0.00	78.05		15	3.86	41.49
	35	0.00	451.93		35	4.85	119.54		35	15.00	68.05
	60	0.00	624.07		60	13.01	140.01		60	33.39	98.82
3%	0	0.00	87.77	3%	0	0.00	10.97	3%	0	0.00	3.25
	1	0.00	87.77		1	0.00	10.97		1	0.00	4.49
	2	0.00	87.77		2	0.00	15.15		2	0.28	6.88
	5	0.00	87.77		5	0.00	19.20		5	1.53	10.06
	15	0.00	121.21		15	5.15	33.95		15	8.80	23.07
	35	0.00	153.63		35	17.93	58.21		35	25.47	47.18
	60	7.52	185.64		60	37.46	91.12		60	47.09	75.72
20%	0	0.00	19.59	20%	0	0.00	2.45	20%	0	0.00	0.73
	1	0.00	19.59		1	0.00	4.29		1	0.34	2.24
	2	0.00	19.59		2	0.21	5.18		2	0.92	3.39
	5	0.00	27.05		5	1.96	9.33		5	3.35	7.26
	15	1.68	41.43		15	9.23	21.82		15	11.89	18.67
	35	10.90	67.63		35	26.16	45.08		35	29.79	40.66
	60	32.02	103.94		60	48.53	73.51		60	52.68	67.79
50%	0	0.00	4.71	50%	0	0.00	0.59	50%	0	0.00	0.17
	1	0.00	6.51		1	0.33	2.03		1	0.64	1.49
	2	0.00	8.25		2	1.02	3.32		2	1.47	2.68
	5	1.09	11.68		5	3.42	6.90		5	4.08	6.03
	15	7.70	25.01		15	12.16	18.33		15	13.17	16.90
	35	23.41	50.02		35	30.14	40.13		35	31.72	38.42
	60	44.78	78.74		60	53.11	67.15		60	54.98	65.16
90%	0	0.00	3.14	90%	0	0.00	0.39	90%	0	0.00	0.12
	1	0.00	4.34		1	0.50	1.83		1	0.70	1.39
	2	0.27	6.64		2	1.20	3.02		2	1.53	2.52
	5	1.75	10.84		5	3.73	6.56		5	4.21	5.85
	15	8.82	23.40		15	12.51	17.65		15	13.41	16.67
	35	25.21	46.38		35	30.85	39.44		35	31.99	38.08
	60	46.59	75.04		60	53.95	66.31		60	55.29	64.81
Likely not useful				May be useful				Likely useful			
									Likely very useful		

still determined by counting limitations. What is an inherently different philosophy compared to all other prior work is that single uranium particle age-dating constraints aren't solely limited by daughter ^{230}Th counts but are also controlled by the number of parent ^{234}U counts detected. As mentioned earlier, the ^{234}U counts are an inverse scaling factor for the CL constraints of the age-dating measurement, making this methodology able to provide useful age-dating information on single particles that are smaller, younger, and lower enriched than previously envisioned. In fact, the calculated model age CLs for extremely young material can be surprisingly narrow as shown in Table 4. There can be great utility in counting zero ^{230}Th ions (zero age in Table 4) in the presence of hundreds of thousands to even millions of ^{234}U counts. The model data in Table 4 show that the smallest confidence interval widths in age would occur for measurements made as close to the purification date as possible. Scanning the data in Table 4 reveals that the absolute CL widths increase as a particle of a given size and enrichment is measured successively later after the purification date even though the relative CL widths decrease. The age-dating measurement uncertainties are dominated by Poisson statistics at low ^{230}Th counts and become closer to Gaussian uncertainty limits based on combined uncertainties of the counting statistics and RSF uncertainty as the ^{230}Th counts increase, ultimately reaching a theoretical confidence interval width that can be no better than the measured RSF uncertainty (standard deviation 3.6%, 7.1% at 95% confidence). Even for the seemingly large confidence interval widths indicated in Table 4, the age-dating data can still be potentially useful, depending on the question being asked. For example, a 1 μm 3% enriched particle with a seemingly unusable model age 95% CL range of 7.52 to 185.64 years can plausibly be determined to have not been purified within the last several years. Additionally, the Table 4 calculated model age data are strictly for individual uranium particle measurements. The following section will explore how to improve upon these

 This journal is © The Royal Society of Chemistry 2019

Published on 10 June 2019. Downloaded by National Institutes of Standards & Technology on 10/12/2022 10:12:13 PM.

model ages further when multiple individual particle measurements from the same location and with the same isotopic composition are made.

Equivalent spherical diameters

An actual particle may have an irregular shape and void spaces, and the chemical form, density and purity of the uranium in the particle may not be known, so the physical size may not be a good indicator of the uranium content. Instead, the integrated ^{234}U counts that are acquired during an age-dating measurement are used to calculate an equivalent spherical diameter (ESD), which is a convenient way to characterize and compare the mass of uranium sputtered from particles during age-dating measurements. The calculation assumes a fully densified (10.96 g cm^{-3}) spherical UO_2 particle because that will give a minimum diameter. If the chemical form were assumed to be U_3O_8, the diameter would be about 11% larger. The calculation converts the ^{234}U counts to ^{234}U atoms removed by sputtering, taking into account the fraction of sputtering time when ^{234}U is measured (7%), the estimated SIMS efficiency of converting sputtered uranium atoms to detected ions (1%)[17,23] and the isotopic fraction of ^{234}U in the particle (measured separately from the residue after the age-dating measurement). The total uranium atoms are converted to the mass of UO_2, then to a volume based on the assumed bulk density, and finally to the diameter of an equivalent sphere.

Validation of method – standards

The first and most accessible validation of the single particle age-dating methodology described in this work was accomplished with a series of U_3O_8 CRMs. Individual particle age-dating measurement results for CRM U900 are displayed in Fig. 5. As mentioned earlier, the U900 material was separately used for long-term measurements to determine the RSF and related uncertainty that are required to make 'unknown' age-dating measurements. The data in Fig. 5 are a result of applying the age-dating methodology to individual CRM U900 particles when treated as an unknown material. For the U900 material, which is old, highly enriched, and present in relatively large particle sizes, the age-dating measurement is not particularly challenging. Reports in the literature discuss the ability of age-dating single particles with similar characteristics,[8,11] even though the previously published methodologies break down for young, small, and LEU oxide materials. The individual particle age-dating data in Fig. 5 show confidence interval widths that are all similar because they approach the CL widths defined by the RSF uncertainty. Comparing the measured data with the predicted data in Table 4, the interval widths almost perfectly align with the expected age-dating interval widths for particles in the 2 μm to 3 μm size range at 90% enrichment and 60 years of age. The calculated ESDs range from 2.1 μm to 2.9 μm.

A concept that is employed here is the data aggregation of individual particle age-dating measurements. Once it is determined that a population of individual uranium oxide particles from a single location have the same isotopic compositions

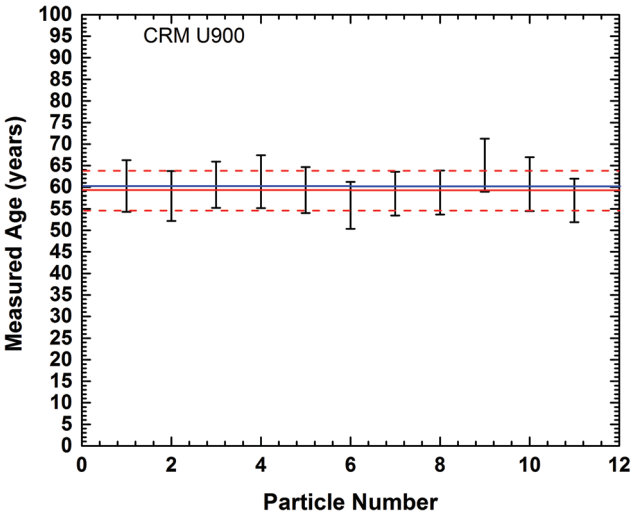

Fig. 5 Plot of measured age in years *vs.* particle number for individually analyzed CRM U900 U_3O_8 particles; black error bars are 95% confidence intervals for individual particle measurements, calculated according to the methodology described in the text; solid red line is the aggregate model age of 59.3 ± 4.4 years using the same calculation method, where dashed red lines are the 95% CLs for the aggregated age; solid blue line is based on the best-known purification date for the CRM material. All ages calculated relative to the analysis date (Table 2). Equivalent spherical diameters: 2.1 to 2.9 μm (average of 2.5 μm).

and that the individual age-dating CLs among the particles overlap, the raw age-dating data can be combined into one set of data as if the measurement were performed on one large particle. By simply summing the ^{230}Th counts and ^{234}U counts from multiple particles and then applying the same age-dating calculations, the result is an aggregate age that will usually have a smaller uncertainty compared to what the individual particle measurements would otherwise suggest. In Fig. 5, the best-known purification date is almost identical to the aggregate age. In this case, the good agreement was expected because longer-term measurements of the same material and its known age were used to determine the RSF. The confidence interval for the CRM U900 aggregate age does not decrease much compared to the individual particle confidence intervals because of the high counts detected for each individual particle. This confidence interval at 54.9 to 63.7 years shown in Fig. 5 compares well with the 55.3 to 64.8 years predicted in Table 4 for a 3 μm (or larger) particle similar in isotopic composition to U900.

In Fig. 6, age-dating measurement validation is demonstrated for six additional CRMs of similar age to U900. The U350, U500, U750, and U970 single particle age-dating measurements are similar to the Fig. 5 U900 CRM data in that (1) there are sufficient ^{230}Th counts that the dominant uncertainties are close to the RSF uncertainty for each individual particle and for the aggregate age measurements, and (2) the aggregate age values agree well with the known purification or shipment dates of the original CRMs, which are contained within the aggregate age CLs. Also in Fig. 6, we present more challenging age-dating measurements than those made on the more highly enriched CRMs by displaying data from U100

Published on 10 June 2019. Downloaded by National Institutes of Standards & Technology on 10/12/2022 10:12:13 PM.

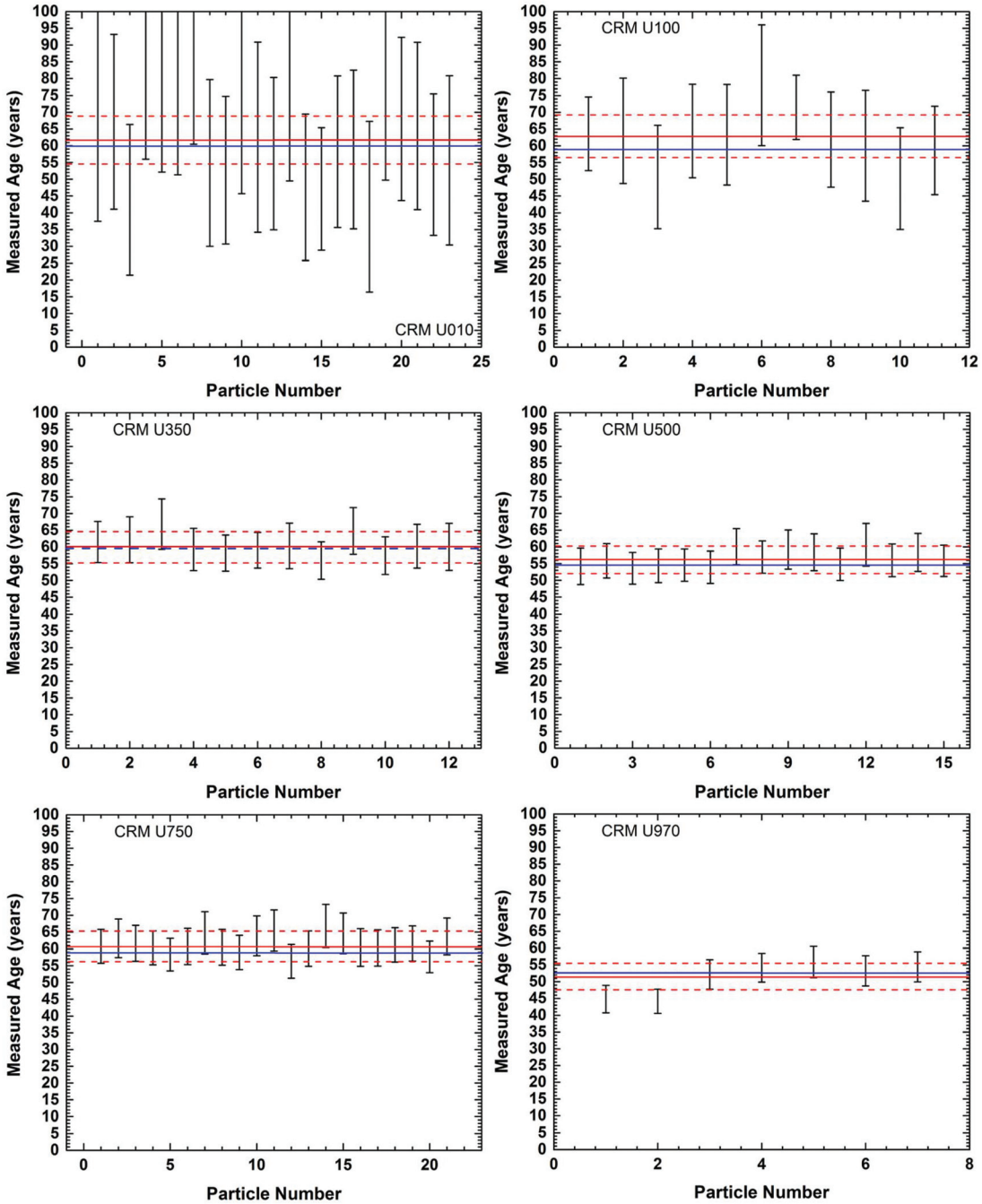

Fig. 6 Plots of measured age in years *vs.* particle number for individually analyzed CRM U010, U100, U350, U500, U750, and U970 U_3O_8 particles; black error bars are 95% confidence intervals for individual particle measurements, calculated according to the methodology described in the text; solid red lines are the aggregate model ages of 61.8 ± 6.8, 62.9 ± 6.1, 59.9 ± 4.7, 56.1 ± 4.0, 60.8 ± 4.4, and 51.5 ± 3.8 years, respectively, using the same calculation method, where dashed red lines are the 95% CLs for the aggregated ages; solid or dashed blue lines are based on the best-known purification dates (or original shipment dates) for each CRM material. All ages calculated relative to the measurement dates (Table 2). Equivalent spherical diameters: U010 – 2.8 to 3.9 μm (average of 3.5 μm), and U100 – 1.9 to 3.0 μm (average of 2.2 μm), U350 – 2.2 to 2.8 μm (average of 2.5 μm), U500 – 2.3 to 3.5 μm (average of 2.9 μm), U750 – 2.5 to 3.9 μm (average of 3.1 μm), and U970 – 2.1 to 3.3 μm (average of 2.7 μm).

(10% enriched material) and U010 (1% enriched material). Both are of similar age to the other CRMs, but the lower ^{234}U abundances yield far fewer ^{234}U atoms than the higher-enriched CRMs. In both the U010 and U100 data in Fig. 6, the individual particle age-dating measurements might be initially interpreted as not particularly useful because of the large 95% confidence intervals. However, aggregate ages of the particles are nearly as precise as those of higher-enriched material. For the U100 particle data, a comparison to the predicted model age confidence intervals in Table 4 implies that the individual

 This journal is © The Royal Society of Chemistry 2019

Published on 10 June 2019. Downloaded by National Institutes of Standards & Technology on 10/12/2022 10:12:13 PM.

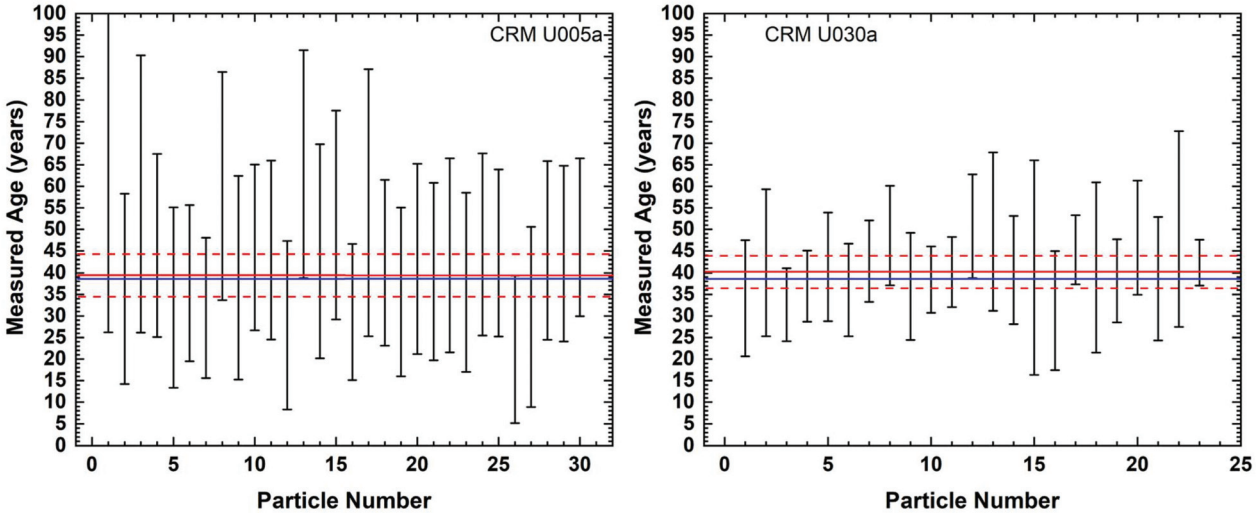

Fig. 7 Plots of measured age in years *vs.* particle number for individually analyzed CRM U005a and U030a U_3O_8 particles; black error bars are 95% confidence intervals for individual particle measurements, calculated according to the methodology described in the text; solid red lines are the aggregate model ages of 39.5 ± 4.8 and 40.2 ± 3.7 years, respectively, using the calculation method described in the text, where dashed red lines are the 95% CLs for the aggregated ages; solid blue lines are the model ages based on bulk isotope dilution measurements for each CRM material.[21] All ages calculated relative to the measurement dates (Table 2). Equivalent spherical diameters: U005a – 3.0 to 4.6 μm (average of 4.0 μm), and U030a – 1.8 to 4.2 μm (average of 2.9 μm).

particle data in Fig. 6 are from 2 μm to 3 μm particles. The calculated ESDs range from 1.9 μm to 3.0 μm. For the U010 data, a similar comparison to Table 4 predicted confidence intervals suggests that the U010 single particle measurements in Fig. 6 are from particles greater than 3 μm in diameter. The ESDs range from 2.8 μm to 3.9 μm.

The final set of method validation data on standards is shown in Fig. 7 for CRMs U005a (0.5% depleted material) and U030a (3% enriched material). These two materials are generally more challenging for age-dating than the U010 and U100 particles because they are each reissued CRMs that are significantly younger. Similar to the U010 and U100 Fig. 6 data, the individual particle age-dating measurements produce large confidence intervals in model age, but the aggregate model ages are very close to the bulk-measured model ages[21] that are within the aggregate CLs. Note that the bulk model ages for these two materials as determined by isotope dilution mass spectrometry are about two years older than expected from the known purification dates. The difference has been attributed to residual ^{230}Th remaining after purification.[21] Compared to the Table 4 predicted model age confidence intervals, the U030a material was likely made up of approximately 3 μm particles, while the even more challenging U005a measurements were likely made on particles greater than 3 μm in diameter.

Validation of method – uraninite

Additional single particle age-dating measurements were made on particles of the mineral uraninite (essentially UO_2) from Topsham, Maine. A slight modification was made to the experimental procedure timing sequence to measure multiple radiochronometers as follows: ^{230}Th – 5 s, ^{231}Pa – 15 s, ^{234}U – 5 s for 20 cycles. The O^- primary ion current in Köhler mode was about 16 nA and produced a ^{234}U count rate of several hundred counts per second. All other details of the age-dating methodology described earlier were the same. The ^{230}Th/^{234}U ratios were calculated taking into account the RSF, but an age calculation based on this ratio is not meaningful for a mineral sample because the ratio should have reached its secular equilibrium value. Instead, the individual particle ^{230}Th/^{234}U ratios are plotted in Fig. 8 with their expanded uncertainties that include contributions from both counting statistics and the

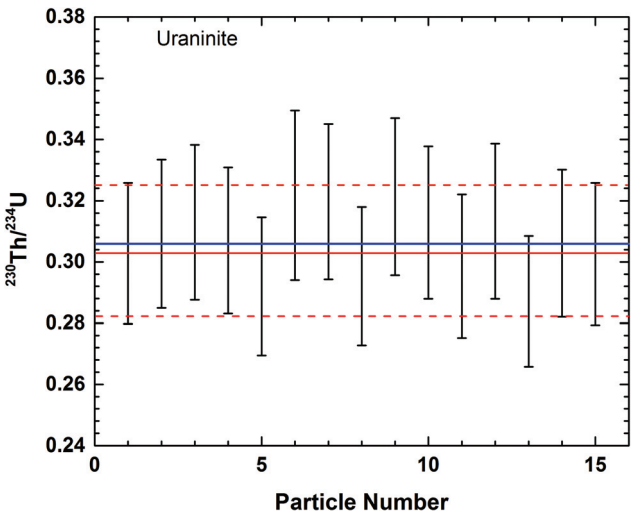

Fig. 8 ^{230}Th/^{234}U ratios measured on individual uraninite particles; error bars are expanded uncertainties at 1.96× standard deviation of each measurement; solid red line is aggregated ratio (0.303 ± 0.022) with 95% expanded uncertainties as red dashed lines; blue line is theoretical ratio of 0.306 under secular equilibrium.

Published on 10 June 2019. Downloaded by National Institutes of Standards & Technology on 10/12/2022 10:12:13 PM.

RSF uncertainty. The aggregated mean ratio plotted as a solid red line is 0.303 with an expanded uncertainty of 0.022 shown in dotted red lines. The expected ratio value assuming secular equilibrium is 0.306. The excellent agreement between the measured and theoretical ratios indicates that the particle measurements provide valid results even in this extreme case. Additionally, the close agreement between measured and theoretical ratios demonstrates the consistency of the measured RSF across multiple uranium oxides since the uraninite is a predominantly UO_2-based material and the U900 CRM used to measure the RSF is U_3O_8.

The $^{231}Pa^+/^{234}U^+$ ratios were also measured for each particle in this experiment. The aggregated ratio was 4.95×10^{-3} with a relative standard deviation of 1.8%. The daughter/parent ion ratio $^{231}Pa^+/^{235}U^+$ is therefore 3.75×10^{-5} based on the natural isotopic abundances of ^{234}U (0.0054%) and ^{235}U (0.720%). The radioactive decay constants of ^{231}Pa and ^{235}U are 2.11×10^{-5} per year and 9.85×10^{-10} per year, respectively, so in secular equilibrium the ratio $^{231}Pa/^{235}U$ is 4.66×10^{-5}. Therefore, in this experiment the Pa/U RSF is determined to be 0.795 ± 0.055 (1σ), compared with the Th/U RSF of 0.673 ± 0.024 (1σ) that was determined from U900 over several hundred measurements. The Pa/U RSF could potentially be used to provide an independent SIMS-based radiochronometer for particles; however, the much lower $^{231}Pa^+$ signal compared with $^{230}Th^+$, about a factor of 40 lower in this case, means that it is not likely to be useful for micrometer-sized particles.

Validation of method – round robin test material

The final validation of the age-dating measurement for the methodology described herein was conducted using the two separate HEU metal materials from the previously described ITWG exercise,[20] with results shown in Fig. 9. These samples were challenging because they were much younger than the CRMs (Sample A – 15.3 years and Sample B – 14.6 years as of the analysis dates, respectively). Sample B data consisted of individual particles that ranged in ESD from 0.9 μm to 6.8 μm with an average of 3.9 μm. Sample A consisted of significantly smaller particles overall, ranging from 0.6 μm to 1.7 μm ESDs, with an average of 0.9 μm. Both Sample A and Sample B individual particle age-dating confidence intervals compare well with those predicted in Table 4 for 15-year-old 90% enriched uranium material. Despite the Sample A and Sample B ITWG particle challenges (young material of small particle size), this new age-dating methodology provides accurate aggregate age data with relatively low uncertainties that would be quite useful for nuclear forensics purposes. Additionally, several of the individual particles from Sample B and a few from Sample A have sufficiently small uncertainties to be useful alone, depending upon the requirements of an investigation. We can estimate the total mass of uranium consumed to acquire the aggregated measurements for these samples based on the integrated ^{234}U counts with adjustments for detection efficiency, isotopic composition and duty cycle. For the 29 particles of Sample A, the total uranium mass consumed is estimated to be about 140 pg, and for the 19 particles of Sample B it is estimated to be approximately 9 ng. These masses are 5 or 6 orders of magnitude smaller than the typical requirements for bulk age-dating measurements by mass spectrometry, albeit that the bulk measurements will have considerably smaller uncertainties.[14,20,21]

It is perhaps surprising that these age-dating measurements give results that are concordant with the casting dates

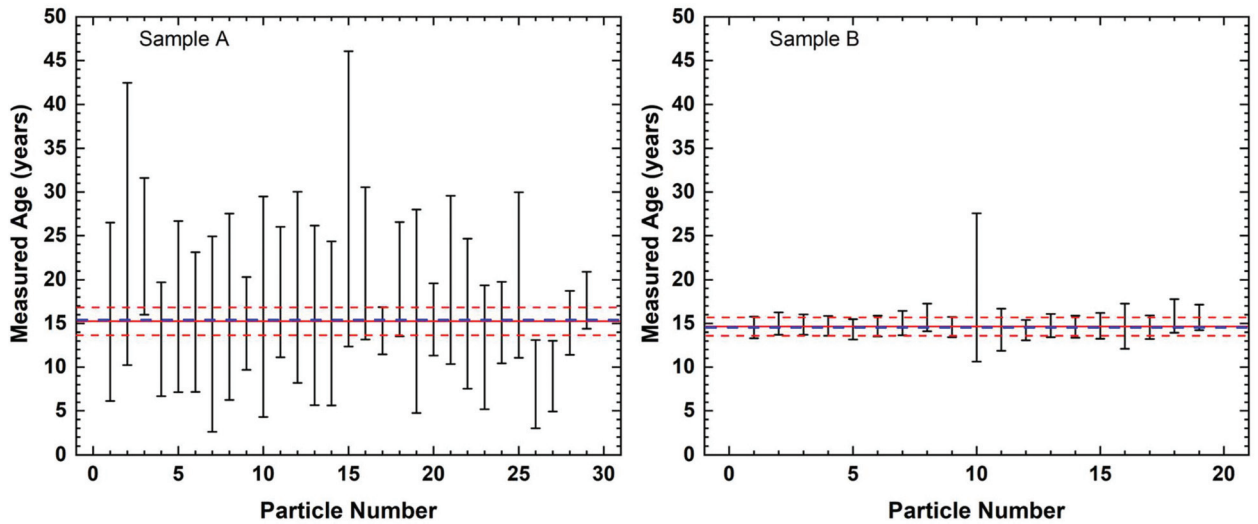

Fig. 9 Plots of measured age in years *vs.* particle number for individually analyzed 'Sample A' and 'Sample B' oxidized uranium particles; black error bars are 95% confidence intervals for individual particle measurements, calculated according to the methodology described in the text; solid red lines are the aggregate model ages of 15.2 ± 1.6 and 14.7 ± 1.1 years, respectively, using the same calculation method, where dashed red lines are the 95% CLs for the aggregated ages; dashed blue lines are based on the known casting dates for each material. All ages calculated relative to the measurement dates (Table 2). Equivalent spherical diameters: Sample A – 0.6 to 1.7 μm (average of 0.9 μm), and Sample B – 0.9 to 6.8 μm (average of 3.9 μm).

 This journal is © The Royal Society of Chemistry 2019

Published on 10 June 2019. Downloaded by National Institutes of Standards & Technology on 10/12/2022 10:12:13 PM.

because the uranium feed material for the casting operation (often UF_4) may have been purified at a much earlier time and will have its own ingrown ^{230}Th. These results indicate that almost all of the thorium must have been expelled from the molten uranium and it presumably diffused to the top of the melt where it would have been trapped in the slag layer.[14]

Possible artifacts

As with all radiochronometers, the specific case studied herein assumes a 'closed system' in that a complete separation of thorium from uranium is made at time zero and that no additional thorium from another source enters into the system, and likewise no thorium or uranium leaves the system. To bias the age-dating measurement 'low' would require thorium removal from a solid sample, which is generally thought to be extremely difficult, although not impossible.[14] Theoretically, thorium species can be removed from a solid sample relative to uranium species through selective solubility in a miscible solvent. This event could cause a chemical state change (voiding the closed system requirement), perhaps resulting in a 'dissolved' or 'melted' look to the particle morphology. Other scenarios that could bias the measurement low, such as an incorrect mass calibration of the measured ^{230}Th peak position, an incorrect assessment of the RSF, or an overcorrection of background noise are eliminated through proper instrumental setup, including the use of daily standards, as well as proper adjustment and review of measurement parameters. Additionally, ejection loss of recoil ^{230}Th during the decay event is theoretically possible, but the recoil range is only tens of nanometers in a uranium matrix, which would be negligible for the micrometer-sized particles of interest because it would only be relevant in the near-surface region. The measurement could be biased high in more plausible ways, such as an incomplete removal of the daughter isotope at time zero. Additionally, adventitious mineral contamination that contains uranium can add ^{230}Th to the measured particle. The uranium isotopic measurement, in which ^{232}Th is measured as part of the isotope sequence, can provide a qualitative indication of significant mineral content, especially if the counts show that the ^{232}Th content is greater than 10^{-4} relative to the total uranium content. The presence of radiogenic lead in the sample, which can be checked by SIMS, would also be an indicator of an unpurified natural uranium component.[24] One also needs to be careful in special cases in which samples come from locations where segregated ^{230}Th can exist, such as the slag from a metal casting operation or debris from the inside of a UF_6 cylinder. In these situations, the model age could appear to be unrealistically high without any indicators of mineral contamination. Other operations such as selective dissolution during solvent extraction or melting and then re-solidifying uranium during metal casting may result in the removal or segregation of thorium, but the degree of purification may not be as high as for one of the UF_6 processes.

Conclusions

We have presented an advanced age-dating measurement procedure for determining the ages of single micrometer-sized uranium-containing particles by large geometry secondary ion mass spectrometry. This methodology incorporated new statistical considerations for the proper interpretation of such data, including the ability to provide meaningful age constraints for particles that do not result in the detection of any ^{230}Th daughter ions. Included was the introduction of the concept of data aggregation of individual particle age data from similar isotopic compositions to reduce age-dating uncertainties. We validated this methodology on multiple uranium oxide CRMs, a uraninite mineral, and particles from cast uranium metal with a full range of depleted through HEU isotopic compositions and a wide range of known purification ages. Additionally, we provided the results of a predictive model that provides guidance on the expected 95% CLs for ages across a multitude of uranium oxide particle sizes, ages, and enrichments so that age-dating measurements can be placed in the proper perspective and the quality of results can be anticipated. The outcome is a significant advance in the age-dating of single uranium-containing particles where this methodology enables the age-dating of particles that are younger, smaller, and at lower enrichments than previously envisioned, and are directly relevant to the International Atomic Energy Agency (IAEA) and its mission to safeguard nuclear materials and monitor member state nuclear programs.

Conflicts of interest

There are no conflicts to declare.

Acknowledgements

The authors thank Drs Joseph Menapace, S. Michael Zemyan, Kevin Coakley, and Charles Brennan for useful discussions about the potential for the measurements made in this work.

References

1 D. L. Donohue and R. Zeisler, *Anal. Chem.*, 1993, **65**, 359A.
2 D. L. Donohue, *IAEA Bull.*, 2002, **44**(2), 17.
3 D. L. Donohue, *J. Alloys Compd.*, 1998, **271–273**, 11.
4 A. Axelsson, D. M. Fischer and M. V. Penkin, *J. Radioanal. Nucl. Chem.*, 2009, **282**, 725.
5 M. Betti, G. Tamborini and L. Koch, *Anal. Chem.*, 1999, **71**, 2612.
6 V. Stebelkov, A. Grachev, A. Ermakov and S. Simakin, *IAEA Safeguards Symposium*, 2010, IAEA-CN-184/083.
7 Yu. V. Stebelkov, M. E. Aleshin, I. A. Elantyev, A. S. Grachev and V. A. Stebelkov, *IAEA Safeguards Symposium*, 2014, IAEA-CN-220/215.

Published on 10 June 2019. Downloaded by National Institutes of Standards & Technology on 10/12/2022 10:12:13 PM.

8 A.-L. Fauré and T. Dalger, *Anal. Chem.*, 2017, **89**, 6663.
9 IAEA Safeguards Research and Development Plan – Enhancing Capabilities for Nuclear Verification, STR-385, January 2018, p. 11.
10 Global Fissile Material Report 2008 – Scope and Verification of a Fissile Material (Cutoff) Treaty, International Panel on Fissile Materials, 2008 Appendix 4A.
11 A. Glaser and S. Bürger, *J. Radioanal. Nucl. Chem.*, 2009, **280**, 85.
12 C. Brennan, C. Szakal, D. Simons and J. Fassett, *IAEA Safeguards Symposium*, 2018, IAEA-CN-267/319.
13 https://en.wikipedia.org/wiki/Bateman_equation accessed, April 25, 2019.
14 M. J. Kristo, A. M. Gaffney, N. Marks, K. Knight, W. S. Cassata and I. D. Hutcheon, *Annu. Rev. Earth Planet. Sci.*, 2016, **44**, 555.
15 K. Mayer, M. Wallenius and Z. Varga, *Chem. Rev.*, 2013, **113**, 884.
16 Certain commercial equipment, instruments or materials are identified in this paper to specify the experimental procedure adequately. Such identification is not intended to imply recommendation or endorsement by the National Institute of Standards and Technology, nor is it intended to imply that the materials or equipment identified are necessarily the best available for the purpose.
17 Y. Ranebo, P. M. L. Hedberg, M. J. Whitehouse, K. Ingeneri and S. Littmann, *J. Anal. At. Spectrom.*, 2009, **24**, 277.
18 D. S. Simons and J. D. Fassett, *J. Anal. At. Spectrom.*, 2017, **32**, 393.
19 P. Croatto, *U Series Reference Material Production, Age, and Sourcing*, New Brunswick Laboratory, 2014.
20 R. Hanlen, *Round Robin 3 Exercise After Action and Lessons Learned Report*, Nuclear Forensics International Technical Working Group (ITWG), April 25, 2011, PNNL-20079.
21 R. W. Williams, A. M. Gaffney, M. J. Kristo and I. D. Hutcheon, *230Th-234U Model-Ages of Some Uranium Standard Reference Materials*, May 28, 2009, LLNL-CONF-413413.
22 G. J. Feldman and R. D. Cousins, *Phys. Rev. D*, 1998, **57**, 3873.
23 N. Sharp, J. D. Fassett and D. S. Simons, *J. Vac. Sci. Technol., B: Nanotechnol. Microelectron.: Mater., Process., Meas., Phenom.*, 2016, **34**, 03H115.
24 A. Fahey, N. Ritchie, D. Newbury and J. Small, *J. Radioanal. Nucl. Chem.*, 2010, **284**, 575.

This journal is © The Royal Society of Chemistry 2019